Synthesis, Reactivity and Molecular Structures of Bis(diphenylphosphanyl)methane-Bridged Heterobimetallic Iron−Platinum Isocyanide Complexes: Breaking and Formation of Metal−Metal Bonds

Michael Knorr,*[a] Isabelle Jourdain,[a] Grégorio Crini,[a] Katja Frank,[b] Hermann Sachdev,[b] and Carsten Strohmann[c]

Keywords: Heterobimetallics / Isocyanide ligands / Metal−metal interactions / Iron / Platinum

When [(OC)$_3$Fe(μ-CO)(μ-dppm)PtCl$_2$] (**1**) is allowed to react with stoichiometric amounts of various isocyanides, cleavage of the metal–metal bond occurs, yielding the heterodinuclear isocyanide complexes [(OC)$_4$Fe{μ-dppm}Pt(Cl)$_2$(CNR)] (**2a**: R = 2,6-xylyl; **2b**: R = *o*-anisyl; **2c**: R = benzyl; **2d**: R = cyclohexyl; **2e**: R = tosylmethyl). Reduction of **2a**–**2e** by NaBH$_4$ in the presence of PPh$_3$ affords the isocyanide-bridged complexes [(OC)$_3$Fe(μ-C=N–R)(μ-dppm)Pt(PPh$_3$)] (**3a**: R = 2,6-xylyl; **3b**: R = *o*-anisyl; **3c**: R = benzyl; **3d**: R = cyclohexyl; **3e**: R = tosylmethyl). Metathesis of **2a**–**2d** with NaI rapidly results in the formation of [(OC)$_4$Fe{μ-dppm}PtI$_2$(CNR)] (**4a**–**4d**), which is slowly transformed under extrusion of CO giving [(OC)$_2$IFe{μ-dppm}(μ-CO)PtI(CNR)] (**6a**: R = 2,6-xylyl; **6b**: R = *o*-anisyl; **6c**: R = benzyl; **6d**: R = cyclohexyl), bearing an iodine ligand at the iron center. Due to this intramolecular iodide migration from Pt to Fe, an Fe^{I} d^{7} fragment interacts with a Pt^{I} d^{9} fragment through a covalent bond. Alternatively, **6a**–**6d** are obtained by stoichiometric treatment of [(CO)$_3$Fe(μ-I)(μ-dppm)PtI] (**5**) with CNR. Single-crystal X-ray diffraction studies are performed on **2d**, **2e** and **3c** as well as on **6d**. In the solid state, the two metal centers of **2e** remain in close contact (3.862 Å), whereas in the case of **2d** they are separated by 6.573 Å after cleavage of the metal–metal bond by CNR.

Introduction

The continuing interest in the preparation and reactivity of heterometallic complexes results from the possibility to investigate (i) cooperativity effects between the different metal centers, (ii) metallosite selectivity on reaction with substrate molecules, and comparison with the reactivity of related monometallic complexes and (iii) possible correlations between unusual bonding modes of coordinated ligands and their activation.[1−10] As part of our studies on the coordination and activation of isocyanide ligands on heterodimetallics,[11−16] we have recently shown that heterodinuclear isocyanide-bridged complexes [(OC)$_3$Fe(μ-C=N−R)(μ-dppm)Pt(PPh$_3$)] with aromatic substituents R (R = 2,6-xylyl, *o*-anisyl, *p*-anisyl; *p*-C$_6$H$_4$NH$_2$) can be obtained by treatment of [(OC)$_3$Fe{Si(OMe)$_3$}(μ-dppm)-Pt(H)(PPh$_3$)] with CNR.[15] Alternatively, some bis(diphenylphosphanyl)amine-bridged complexes [(OC)$_3$Fe(μ-C=N−R)(μ-dppa)Pt(PPh$_3$)] were prepared by selective substitution of the bridging carbonyl ligand of [(OC)$_3$Fe(μ-C=O)-(μ-dppa)Pt(PPh$_3$)] by CNR.[13]

In contrast to the well-established μ-CNR bonding mode for homodimetallic systems,[17,18] this bonding mode is extremely rare for heterometallic systems,[19] therefore, we are interested in developing synthetic methods for [M-(μ-C=N−R)M′] complexes. Here, we report on the reactivity of [(CO)$_3$Fe(μ-CO)(μ-dppm)PtCl$_2$] (**1**) towards various isocyanides, intramolecular redox reactions due to migration of iodo ligands between two adjacent metal centers, and present the molecular structures of several Fe−Pt compounds ligated by terminal or bridging CNR ligands.

Results and Discussion

Reactivity of 1 towards Isocyanides

Since it is easy to substitute the bridging carbonyl ligand of [(OC)$_3$Fe(μ-C=O)(μ-dppa)Pt(PPh$_3$)] by CNR (see above), it seemed promising to prepare [(CO)$_3$Fe{μ-CNR}(μ-dppm)PtCl$_2$] using Shaw's compound [(CO)$_3$Fe{μ-CO}(μ-dppm)PtCl$_2$] (**1**) as the starting material.[20] For the latter compound, the presence of a semi-bridging carbonyl ligand has been established both in solution and in the solid

---

[a] Laboratoire de Chimie des Matériaux et Interfaces, Université de Franche-Comté, Faculté des Sciences et des Techniques,
16, Route de Gray, 25030 Besançon Cedex, France
E-mail: michael.knorr@univ-fcomte.fr
[b] Institut für Anorganische Chemie der Universität des Saarlandes,
Postfach 151150, 66041 Saarbrücken, Germany
[c] Institut für Anorganische Chemie der Universität Würzburg,
Am Hubland, 97074 Würzburg, Germany

state. Instead of the anticipated CO substitution reaction, instantaneous opening of the dative iron→platinum bond occurred at ambient temperature on addition of stoichiometric amounts of RNC to a CH_2Cl_2 solution of **1**. The resulting complexes [$(OC)_4Fe\{\mu\text{-dppm}\}Pt(Cl)_2(CNR)$] (**2a**: R = 2,6-xylyl; **2b**: R = *o*-anisyl; **2c**: R = benzyl; **2d**: R = cyclohexyl; **2e**: R = tosylmethyl) (Scheme 1) were isolated in high yields as yellow solids, which can be handled in air without significant decomposition. They show poor solubility in hexane or Et_2O, but are very soluble in THF or dichloromethane.

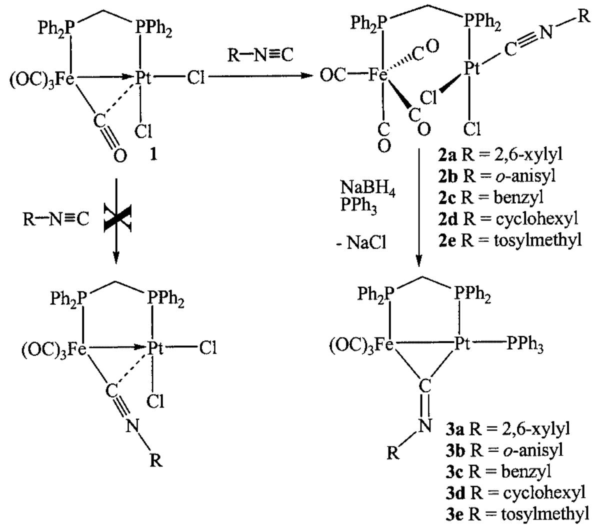

Scheme 1

The IR spectrum of **2a** indicates the breaking of the Fe−Pt bond. The pattern and position of the four ν(CO) stretching modes at 2051, 1978, 1942 and 1936 cm^{-1} in the IR spectrum is very similar to that of [$(OC)_4Fe(\eta^1\text{-dppm})$].[21] The ν(C≡N) vibration at 2199 cm^{-1} is assigned to the terminally bound isocyanide ligand on Pt. Due to the absence of a metal−metal bond, the $^2J_{P,P}$ coupling of the two doublets found at δ = 64.5 (P_{Fe}) and 2.9 ppm (P_{Pt}) in the $^{31}P\{^1H\}$ NMR spectrum, is reduced to 26 Hz compared with 51 Hz reported for **1**. The data of all other derivatives are very similar and are listed in Table 1. The $^{195}Pt\{^1H\}$ NMR spectra of **2a**, **2b** and **2e** give rise to broadened doublets at δ ≈ −2400 ppm, whose $^3J_{Pt,P}$ coupling is not resolved. This is in contrast to the sharp resolved $^{31}P\{^1H\}$ NMR spectra that exhibit a $^3J_{Pt,P}$ coupling of ca. 90 Hz, in addition to an averaged $^1J_{Pt,P}$ coupling of 3300 Hz. The cleavage of the Fe−Pt bond of **2d** and **2e** was further corroborated by an X-ray diffraction study.

Crystal Structures of [$(OC)_4Fe\{\mu\text{-dppm}\}PtCl_2(CNCH_2SO_2C_6H_4Me)$]·0.5$CH_2Cl_2$ (2e) and [$(OC)_4Fe\{\mu\text{-dppm}\}PtCl_2(CNC_6H_{11})$] (2d)

Suitable crystals of **2e**·0.5CH_2Cl_2 were grown from CH_2Cl_2/Et_2O. The molecular structure is shown in Figure 1 with selected bond lengths and angles. The cleavage of the metal−metal bond by the isocyanide ligand is shown by the separation of 3.862 Å between the iron center and the platinum center. The angle P(2)−C(17)−P(1) of 121.7(3)° is larger than in the case of $(CO)_3Fe\{\mu\text{-C=N-benzyl}\}(\mu\text{-dppm})Pt(PPh_3)$] (**3c**), for which a P−C−P angle of 112.8(2)° is found (see below). The coordination sphere around Pt is square-planar, the root mean square deviation from the plane defined by Cl(1), Cl(2), P(2), C(30) and Pt is quite small (0.045 Å). The two chlorine atoms are in a *cis* arrangement [Cl(1)−Pt−Cl(2) = 90.64(10)°], the angles P(2)−Pt−Cl(1) and P(2)−Pt−Cl(2) are 84.93(8)° and 175.53(7)°, respectively. The two Pt−Cl bond lengths of 2.331(2) Å and 2.350(2) Å are very similar. The Pt−P(2) and Fe−P(1) distances of 2.253(2) Å and 2.256 Å are comparable to those found in **3c**. The Pt−C(30)−N−C(31) array of the terminally bound isocyanide ligand {*d*[C(30)]−N = 1.164(11) Å}, having angles of 178.2(7)° and 173.7(9)°, is almost linear. The geometry around the iron center can be described as a weakly deformed trigonal bipyramid, in which the angle C(2)−Fe−P(1) [171.7(4)°] of

Table 1. Selected $^{31}P\{^1H\}$ and $^{195}Pt\{^1H\}$ NMR data (δ in ppm and *J* in Hz)

Complex	$\delta(P_{Fe})$	$\delta(P_{Pt})$	$\delta(PPh_3)$	$^2J_{P,P}$, $^2J_{P,P}$; $^1J_{Pt,P}$, $^3J_{Pt,P}$	$\delta(^{195}Pt)$
2a	64.5 d	2.9 d		26; 3344, 82	−2387 d, br.
2b	64.9 d	3.0 d		26; 3336, 83	−2400 d, br.
2c	64.9 d	3.9 d		23; 3360, 95	
2d	64.3 d	4.0 d		25; 3392, 99	
2e	64.4 d	3.8 d		23; 3271, 96	−2431 d, br.
3a	73.6 dd	32.7 dd	42.0 dd	152, 5, 27; 4266, 2527, 75	−2586 ddd
3b	71.3 dd	30.7 ff	41.6 dd	152, 5, 28; 4188, 2549, 69	−2594 ddd
3c	71.1 dd	30.1 dd	40.8 dd	156, 4, 28; 4208, 2570, 64	−2608 ddd
3d[a]	72.7 d	30.7 dd	39.9 d	155, 31; 4247, 2541, 66	
3e	69.5 dd	28.7 dd	39.3 dd	144, 6, 25; 4129, 2516, 66	−2580 ddd
4b	66.5 d	−1.0 d		28; 3168, 73	
4c	66.7 d	0.6 d		27; 3185, 84	
4d	66.4 d	1.5 d		26; 3219, 96	
6b	49.1 d	6.4 d		75; 3163, 151	
6c	50.4 d	7.2 d		74; 3159, 152	
6d	50.4 d	7.5 d		75; 3175, 152	

[a] T = 243 K.

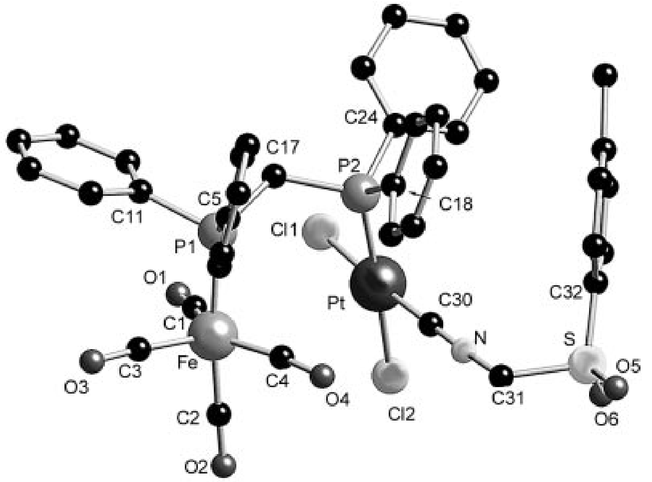

Figure 1. View of the crystal structure of **2e** showing the atom numbering scheme; selected bond lengths [Å] and angles [°]: Pt−C(30) 1.876(8), C(30)−N 1.164(11), C(31)−N 1.386(11), Pt−Cl(1) 2.331(2), Pt−Cl(2) 2.350(2), Pt−P(2) 2.253(2), P(2)−C(17) 1.832(6), P(1)−C(17) 1.844(7), Fe−P(1) 2.256(2), Fe−C(1) 1.791(10), Fe−C(2) 1.774(10), Fe−C(3) 1.801(9), Fe−C(4) 1.778(8), C(1)−O(1) 1.156(12), C(2)−O(2) 1.147(12), C(3)−O(3) 1.144(10), C(4)−O(4) 1.151(10); Cl(2)−Pt−Cl(1) 90.64(10), Cl(1)−Pt−P(2) 84.93(8), Pt−C(30)−N 178.2(7), C(30)−N−C(31) 173.7(9), N−C(31)−S 112.8(7), C(31)−S−C(32) 104.5(4), Cl(1)−Pt−C(30) 175.1(2), C(1)−Fe−C(3) 109.6(4), C(1)−Fe−C(2) 109.6(4), C(1)−Fe−C(4) 139.0(4), C(3)−Fe−C(4) 111.3(4), C(2)−Fe−C(4) 85.4(4), C(1)−Fe−P(1) 88.3(3), C(2)−Fe−P(1) 171.7(4), C(3)−Fe−P(1) 92.2(3), C(4)−Fe−P(1) 92.7(4), Fe−C(1)−0(1) 173.2(9), Fe−C(2)−0(2) 179.0(13), Fe−C(3)−0(3) 176.5(8), Fe−C(4)−0(4) 172.8(7), P(1)−C(17)−P(2) 121.7(3)

the axial ligands deviates slightly from the ideal value. The angles of the equatorial carbonyl ligands deviate considerably from the ideal value of 120°; C(1)−Fe−C(4) and C(1)−Fe−C(3) are 139.0(4) and 109.6(4)°, respectively.

Surprisingly, despite the similarity of the spectroscopic data recorded in solution, the mutual arrangement of the two metal fragments of **2d** in the crystalline state is very different from that of **2e**. Although the geometry and ligand arrangement of each individual moiety remains unaltered (square-planar around Pt and trigonal-bipyramidal around Fe), the two metal centers are far apart from each other (6.573 Å) after cleavage of the metal−metal bond by cyclohexyl isocyanide (see Figure 2). The angle P(2)−C(17)−P(1) [130.1(2)°] is still larger than in the case of **2e**, for which a P−C−P angle of 121.7(3)° is found. Compared with **2e**, the distances Fe−P(1) and Pt−P(2) [2.2565(14) and 2.2540(13) Å, respectively] of **2d** remain almost identical. However, all interligand angles on the iron fragment are now much closer to the values expected for an ideal trigonal-bipyramidal polyhedron. Notably the angles between the equatorial carbonyl ligands C(1), C(2) and C(4) are 123.1(2), 119.8(2) and 117.1(3)°, which are much closer to 120°. Furthermore, the angle P(1)−Fe−C(3) [178.2(2)°] is much closer to 180° than the angle 171.7(4)° found for derivative **2e**.

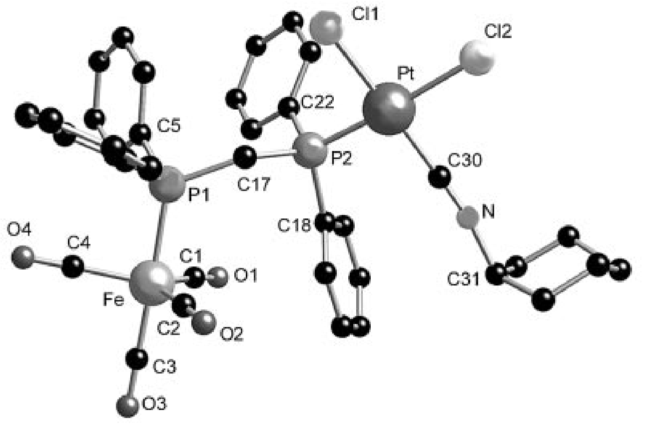

Figure 2. View of the crystal structure of **2d** showing the atom numbering scheme; selected bond lengths [Å] and angles [°]: Pt−C(30) 1.929(3), C(30)−N 1.136(6), C(31)−N 1.489(7), Pt−Cl(1) 2.3218(12), Pt−Cl(2) 2.3615(15), Pt−P(2) 2.2540(13), P(2)−C(17) 1.835(4), P(1)−C(17) 1.860(4), Fe−P(1) 2.2565(14), Fe−C(1) 1.784(5), Fe−C(2) 1.798(6), Fe−C(3) 1.787(5), Fe−C(4) 1.810(5), C(1)−O(1) 1.148(6), C(2)−O(2) 1.137(7), C(3)−O(3) 1.136(7), C(4)−O(4) 1.136(4); Cl(2)−Pt−Cl(1) 89.68(5), Cl(1)−Pt−P(2) 88.81(5), Pt−C(30)−N 178.0(5), C(30)−N−C(31) 171.4(5), Cl(1)−Pt−C(30) 176.9(2), C(1)−Fe−C(3) 88.2(2), C(1)−Fe−C(2) 123.1(2), C(1)−Fe−C(4) 119.8(2), C(3)−Fe−C(4) 90.2(2), C(2)−Fe−C(4) 117.1(3), C(1)−Fe−P(1) 92.45(14), C(2)−Fe−P(1) 89.4(2), C(3)−Fe−P(1) 178.2(2), C(4)−Fe−P(1) 88.0(2), Fe−C(1)−0(1) 175.4(4), Fe−C(2)−0(2) 177.2(5), Fe−C(3)−0(3) 178.6(6), Fe−C(4)−0(4) 178.6(4), P(1)−C(17)−P(2) 130.1(2)

A very similar important separation of the two dppm-spanned metal fragments has recently been encountered, after cleavage of the dative metal−metal bond of [MeCp-$(OC)_2$Mn(μ-CO)(μ-dppm)$PdCl_2$] by isocyanides.[22] In the case of [(η^5)-MeCp$(OC)_2$Mn(μ-dppm)Pd(CNxylyl)Cl_2], an X-ray diffraction study determined a separation of 6.31 Å between the square-planar palladium center and the three-legged piano-stool MeCp$(OC)_2$MnP fragment.

These findings outline the flexibility and the rotational degrees of freedom along the M−P−C−P−M′ chains. At present we cannot state whether the different arrangements of **2d** and **2e** are only due to *packing effects* in the crystalline state, or whether the different *electronic behavior* of the CNR ligands may account for this phenomenon. The C_6H_{11} group is known as electron-releasing, whereas the CH_2SO_2*p*-tolyl group should somewhat lower the electron density on Pt by the enhanced propensity of tosylmethyl isocyanide to act as a π-accepting ligand.[14] In the latter case, the proximity of the two adjacent metal centers and the widening of the angle C(1)−Fe−C(4) to 139.0(4)°, may tentatively be interpreted as *incipient dative metallic interaction* between the iron and platinum fragment. [The closest contacts between Pt and C(4) and C(1) are 3.499 Å and 3.819 Å, respectively.] Examples of heterodimetallic complexes with dative Fe→Pt bonds such as [$(OC)_3$Fe(μ-CO)(μ-dppm)$PtBr_2$] and [$(CO)_3$Fe(μ-I)(μ-dppm)PtI] (**5**) exhibit metal−metal separations of 2.647(4) and 2.523(4) Å, respectively.[20] For the cyclopentadienethiolato compound [$(C_5H_4S)_2$FePdPPh$_3$], which possesses a weak dative Fe→Pd interaction, a value of 2.878(1) Å has been reported.[23] A separation of 3.784 Å, which is quite close to that of **2e**, has been determined for the dppm-spanned complex [Cp(PPh$_3$)Ru(μ-dppm)(μ-Cl)$PtCl_2$].[24] However, in the latter case a bridging chloro ligand additionally links the two moieties. Of course, further molecular structures of derivatives of **2** ligated by strongly π-accepting CNR ligands are necessary to corroborate (or exclude) this hypothesis.

Reduction of 2a−2e Yielding μ-Isocyanide Complexes

Due to the paucity of heterometallic M(μ-C=N−R)M′ systems, it is desirable to develop facile preparative routes to deepen the knowledge on the structural features and reactivity pattern of this class of compounds. We found that apart from the two strategies mentioned in the introduction, Fe(μ-C=N−R)Pt systems are also accessible using **2a−2e** as precursors. When **2a−2b** were reduced by $NaBH_4$ in the presence of 1 equiv. of PPh_3 using a CH_2Cl_2/MeOH mixture as the solvent, the recently described μ-isocyanide complexes $[(CO)_3Fe(\mu\text{-}C{=}N\text{-aryl})(\mu\text{-dppm})Pt(PPh_3)]$ **3a−3b** were isolated after workup in ca. 60% yield. In an analogous manner, the stable complexes **3c−3e**, possessing μ-CNR bridges with aliphatic groups R, have been obtained in moderate yields as yellow-orange solids. The ^{31}P and ^{195}Pt NMR spectroscopic data, which have already been discussed in detail,[15] are listed in Table 1. A comparison of the ν(C=N) vibration in the IR spectra reveals that the position of this absorption can roughly be correlated with the donor/acceptor properties of the group R. Thus, the CH_2SO_2*p*-tolyl substituent, which is the best π-acceptor in this series, gives rise to a ν(C=N) vibration at 1648 cm^{-1}. For R = xylyl and *o*-anisyl a ν(C=N) vibration at 1667 and 1668 cm^{-1}, respectively, has been reported,[15] and for the benzyl derivative a ν(C=N) vibration appears at 1679 cm^{-1}. Finally, in the case of **3d** with a strongly electron-donating C_6H_{11} group, this stretching mode is shifted to 1689 cm^{-1}.

Crystal Structure of $[(CO)_3Fe\{\mu\text{-}C{=}N\text{-}Bz\}(\mu\text{-dppm})Pt(PPh_3)]\cdot 0.5CH_2Cl_2$ (3c)

The molecular structure of the benzyl derivative is depicted in Figure 3 with selected bond lengths and angles. The Fe−Pt distance of 2.5575(10) Å confirms the existence of a metal−metal bond and is almost identical to those of $[(CO)_3Fe(\mu\text{-}C{=}N{-}R)(\mu\text{-dppm})Pt(PPh_3)]$ and $[(CO)_3Fe(\mu\text{-}C{=}O)(\mu\text{-dppm})Pt(PPh_3)]$ [2.579(4) Å].[21] On the whole, there are many parallels in the overall structure, therefore only the most salient structural features of **3c** will be mentioned. The bridging isocyanide ligand is again symmetrically ligated between the two metal centers, the Fe−C(1) and Pt−C(1) distances are 2.040(5) and 1.984(5) Å, respectively. The angle defined by the two planes Fe−P(1)−P(2)−Pt and Fe−C(1)−Pt is 6.02°. The length of the C(1)=N double bond [1.234(6) Å] compares with that of other dimetallic isocyanide-bridged systems. Distances of 1.239(7) and 1.23(3) Å have been reported for $[Ni_2(\mu\text{-dppm})_2\{\mu\text{-}C{=}NMe\}(CNMe)_2]$ and for $[Pd_2(\mu\text{-dppm})_2\{\mu\text{-}C{=}NMe\}(CNMe)_2][PF_6]_2$.[25,26] The C(1)−N−C(2) bending of 122.0(4)° is even more accentuated than in the above-mentioned homodimetallic Ni−Ni [129.9(6)°] and Pd−Pd systems [131.0(2)°], and parallels that of $[Fe_2(\mu\text{-}C{=}NEt)_3(CNEt)_6]$ [123.1(1)°].[27] Due to the bending of the organic group R of the isocyanide bridge, two isomeric forms, with orientation towards Pt or Fe, are conceivable a priori. From Figure 3 it can be seen that from a steric point of view, an orientation of the benzyl group towards the carbonyliron fragment is imposed in order to avoid repulsion with the bulky PPh_3 ligand.

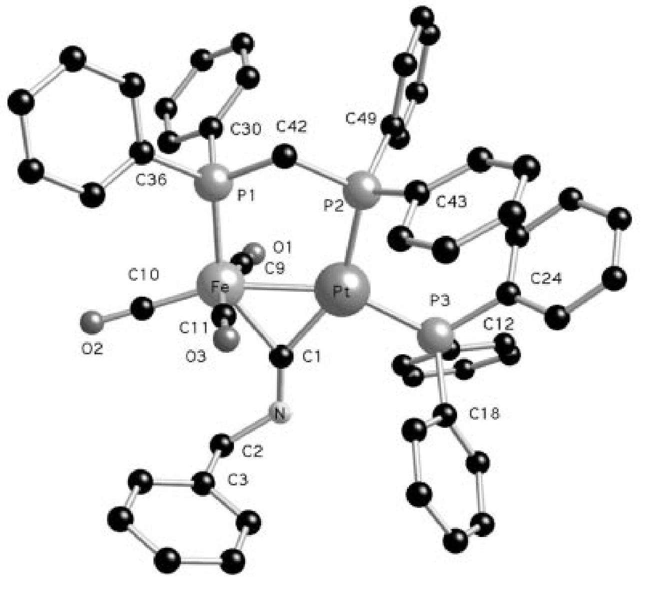

Figure 3. View of the crystal structure of **3c** showing the atom numbering scheme; selected bond lengths [Å] and angles [°]: Fe−Pt 2.5577(10), Fe−P(1) 2.240(2), Pt−P(2) 2.3087(13), Pt−P(3) 2.2632(13), Pt−C(1) 1.984(5), Fe−C(1) 2.040(5), Fe−C(9) 1.788(5), Fe−C(10) 1.762(5), Fe−C(11) 1.786(5), C(1)−N 1.234(6), C(2)−N 1.470(6), C(10)−O(2) 1.150(6), C(10)−O(2) 1.150(6), C(11)−O(3) 1.152(6), P(1)−C(42) 1.854(9), P(2)−C(42) 1.859(5); C(1)−N(1)−C(2) 122.0(4), Pt−C(1)−Fe 78.9(2), Fe−Pt−C(1) 51.51(14), C(1)−Fe−Pt 49.58(12), C(1)−Fe−P(1) 144.08(13), C(1)−Pt−P(2) 148.99(14), C(1)−Pt−P(3) 102.70(14), C(1)−Fe−C(9) 82.1(2), C(1)−Fe−C(10) 110.2(2), C(1)−Fe−C(11) 83.1(2), N−C(1)−Fe 140.0(3), N−C(1)−Pt 140.9(4), P(1)−Fe−Pt 93.63(8), P(2)−Pt−P(3) 107.17(5), Fe−Pt−P(3) 154.18(4), P(1)−C(42)−P(2) 112.8(2)

Iodide Migration from Pt to Fe

With the objective of obtaining additional information on the parameters influencing the structural features of **2,** we tried to prepare the iodo derivatives $[(OC)_4Fe(\mu\text{-dppm})PtI_2(CNR)]$ (**4**) in a metathesis reaction by addition of an excess of NaI to a CH_2Cl_2/THF solution of **2a−2d** according Scheme 2. Surprisingly, **4a** could not be isolated in a pure form. Instead, after 8 h at ambient temperature, and subsequent workup, red-brown crystals were isolated in a 60% yield. The spectroscopic data and elemental analysis were consistent with the formation of the heterodimetallic complex $[(OC)_2FeI(\mu\text{-dppm})(\mu\text{-CO})PtI(\text{Xylyl-CN})]$ (**6a**). Compound **6a** can be described as a dinuclear complex, in which the Fe^I d^7 fragment interacts with the Pt^I d^9 fragment through a covalent Fe−Pt bond. This description, implying the formal oxidation of Fe and reduction of Pt, satisfies an 18-e configuration for Fe and a 16-e configuration for Pt. Mechanistically, this reaction can be rationalized as the migration of a *Pt*-bound iodide ligand to Fe, initiated by the extrusion of a carbonyl ligand (due to the bigger diameter of iodide compared with a chloride ligand). Although an intermolecular ligand transfer cannot be excluded unambiguously, an intramolecular migration seems more probable. This hypothesis is corroborated by the observation that isolated **4c** or **4d** are converted within ca. 8 h quantitatively to **6c**, **6d** after dissolution in CH_2Cl_2. Halide transfer reactions are not unusual in heterodimetallic chemistry.[28−33] For example, the reaction of *cis*-[Pt(DMSO)$_2$Cl$_2$] with [CpRh(CO)(Ph$_2$Ppy)] yielded (via some intermediates) the Rh^{II}−Pt^{I} compound [CpRhCl(μ-Ph$_2$Ppy)Pt(CO)Cl] by mutual CO/chloride exchange.[28]

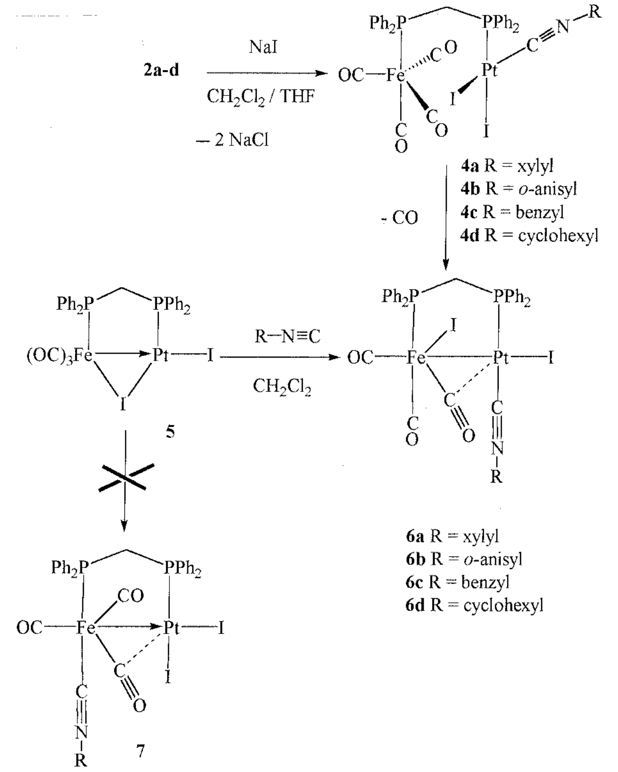

Scheme 2

Spectroscopic Data

^{31}P NMR spectroscopic monitoring of the metathesis reaction of **2b** in a CDCl$_3$/acetone solution revealed the formation of a new species whose chemical shifts [$\delta = 66.5$ (P_{Fe}) and -1.0 (P_{Pt})] and coupling constants ($^{2}J_{P,P} = 28$, $^{1}J_{P,Pt} = 3168$, $^{3}J_{P,Pt} = 73$ Hz) are very similar to those of **2b**, indicating the formation of **4b** as an intermediate. In the course of several hours, a new AX pattern due to **6b** emerged. It consists of two doublets at $\delta = 49.1$ ppm ($^{2+3}J_{P,P} = 75$ Hz), assigned to the *Fe*-bound phosphorus nucleus, and at $\delta = 6.4$ ppm for the *Pt*-bound phosphorus nucleus. All resonance signals are flanked by ^{195}Pt satellites, the Pt−P couplings are 152 and 3159 Hz. After 7 h, **4b** was completely converted to **6b**. The IR spectrum of **4b** (recorded in CH_2Cl_2) exhibits 4 vibrations due to the Fe(CO)$_4$ fragment, whose positions are, as expected, very close to that of **2b**. However, the ν(C≡N) absorption at 2093 cm^{-1} shifts to a lower frequency by 11 cm^{-1}, relative to the chloro precursor **2b**. The IR spectrum of **6b** exhibits two terminal ν(CO) stretching modes at 2013 and 1947 cm^{-1}, a vibration due to a semi-bridging carbonyl ligand is found at 1840 cm^{-1}. The strong absorption at 2189 cm^{-1} is assigned to the ν(CN) stretching mode of the terminally bound isocyanide ligand on Pt.

We were further interested in examining the reactivity of the iodide-bridged complex **5** towards the addition of stoichiometric amounts of isocyanide. This reaction could also a priori lead to **6** by the coordination of CNR on Pt and the formation of a terminal iron−iodine bond. Alternatively, the formation of an isomeric complex of type **7**, bearing a terminal CNR ligand on a formally Fe^{0} center and two iodine ligands on a Pt^{II} center (the two metal atoms connected by a dative metal−metal bond), could be envisaged. However, performing this experiment in dichloromethane at ambient temperature with xylyl-, benzyl- or cyclohexyl isocyanide exclusively afforded **6a**−**6d**, with excellent yields.

It is interesting to compare this reactivity pattern of **5** towards the CNR donor ligand, with the results of Shaw's group who used PPh$_3$. In the latter case, the iodide bridge between the two metal atoms remained intact and the formation of [(CO)$_3$Fe(μ-I)(μ-dppm)Pt(PPh$_3$)I] was observed.[20]

Crystal Structure of [(OC)$_2$FeI(μ-CO)(μ-dppm)PtI(CNC$_6$H$_{11}$)]·CH$_2$Cl$_2$ (6d)

Suitable red-violet crystals were obtained by slow diffusion of heptane into a saturated dichloromethane solution of **6d**. The molecular structure of the cyclohexyl derivative, including the atom numbering scheme is shown in Figure 4 with selected bond lengths and angles. The iron and platinum moieties are linked by a dppm bridge giving a five-membered Fe−P−C−P−Pt ring. The Fe−Pt distance of 2.6981(8) Å confirms the existence of a metal−metal bond, and is close to that of [(OC)$_3$Fe{Si(OMe)$_3$}(μ-dppa)Pt(H)(PPh$_3$)] [2.670(2) Å],[15] but appreciably longer than that of **3c**. The Pt−C(3) distance of 2.250(5) Å and the angles Fe−C(3)−O(3) [158.5(4)°] and Pt−C(3)−O(3) [118.6(3)°] indicate the presence of a semi-bridging carbonyl ligand, as suggested by the IR spectra. The Fe atom is located in a distorted octahedral environment due to the semi-bridging C(3)O(3) group [C(2)−Fe−I(1) 114.7(2)°, C(2)−Fe−C(3) 104.1(2)°]; the P(1) and I(1) atoms are in a mutual *cis* arrangement [I(1)−Fe−P(1) 87.42(4)°], whereas the remaining coordination sites are occupied by the Pt atom and three carbonyl groups. The square-planar geometry around Pt [neglecting the weak Pt−C(3) interaction] is achieved by bonding with Fe, P(2), C(29) and I(2). The latter I atom is *cis* to P(2) [I(2)−Pt−P(2) 90.50(4)°] and *trans* to the Fe−Pt bond [I(2)−Pt−Fe 168.95(2)°], forming a torsion angle I(1)−Fe−Pt−I(2) of 15.44°.

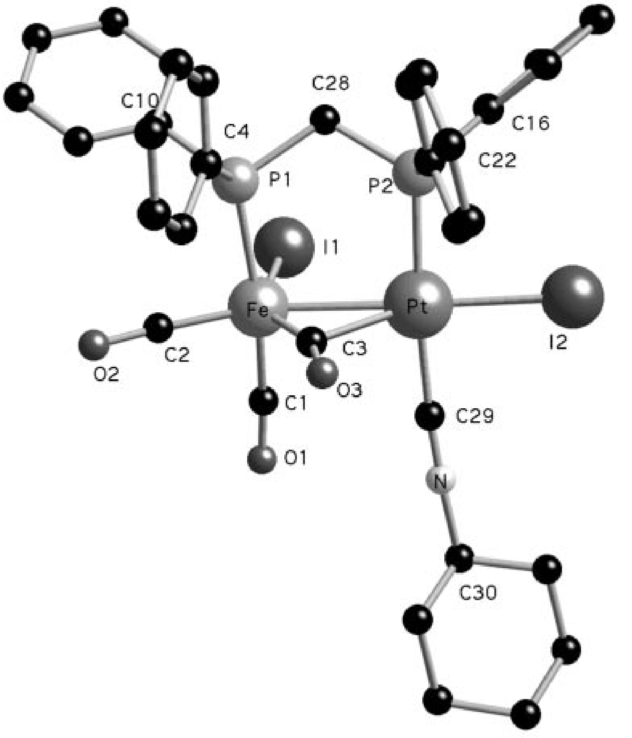

Figure 4. View of the crystal structure of **6d** showing the atom numbering scheme; selected bond lengths [Å] and angles [°]: Fe−Pt 2.6981(8), Fe−I(1) 2.660(5), Fe−P(1) 2.2712(13), Pt−P(2) 2.2891(12), Pt−I(2) 2.6553(6), Pt−C(29) 1.980(5), Pt−C(3) 2.250(5), Fe−C(1) 1.813(6), Fe−C(2) 1.755(6), Fe−C(3) 1.800(4), C(29)−N 1.146(6), C(1)−O(1) 1.130(7), C(2)−O(2) 1.157(7), C(3)−O(3) 1.174(6), P(1)−C(28) 1.822(5), P(2)−C(28) 1.832(4); N−C(29)−Pt 175.6(5), C(29)−N−C(30) 177.4(6), Pt−C(3)−Fe 82.7(2), Fe−Pt−C(29) 93.59(14), I(1)−Fe−Pt 85.40(3), I(2)−Pt−Fe 168.95(2), I(1)−Fe−P(1) 87.42(4), I(2)−Pt−P(2) 90.50(4), C(29)−Pt−P(2) 174.74(13), C(29)−Pt−Fe 93.59(14), C(1)−Fe−C(2) 87.4(2), C(1)−Fe−C(3) 94.2(2), C(2)−Fe−C(3) 104.1(2), O(3)−C(3)−Fe 158.5(4), O(3)−C(3)−Pt 118.6(3), P(1)−Fe−Pt 96.63(4), Fe−Pt−P(2) 91.44(4), P(1)−C(28)−P(2) 111.5(2)

Conclusion

These investigations have shown that **1** is a very useful precursor for the synthesis of heterodimetallic complexes ligated by aliphatic and aromatic isocyanide ligands in a terminal or bridging bonding mode. This study has shown that complexes **2**, resulting from the rupture of the dative Fe→Pt bond of **1**, possess diverging conformations in the crystalline state, depending on the nature of R of the CNR ligand. By varying (i) the steric and electronic properties of R, (ii) the spanning diphosphane ligand and (iii) the substitution of the two *Pt*-bound chloro ligands by other ligands, future studies may elucidate the origin of the different conformations of the Fe−P−C−P−Pt arrays encountered for **2d**, **2e**. Furthermore, the iodo complexes [$(OC)_2FeI(\mu\text{-dppm})(\mu\text{-CO})PtI(RCN)$] (**6**), obtained by intramolecular halide transfer, seem to be promising starting materials for reactivity studies towards unsaturated small molecules, for the transformation of the reactive CN triple bond to other organic functional groups, such as aminocarbenes, as well as for C−C coupling reactions.[17,34−38]

Experimental Section

General: All reactions were performed in Schlenk-tube flasks under purified nitrogen. Solvents were dried and distilled under nitrogen before use, toluene and hexane from sodium, dichloromethane from P_4O_{10}. Nitrogen was passed through BASF R3-11 catalyst and molecular sieve columns to remove residual oxygen and water. IR spectra were recorded with a Nicolet Nexus 470 spectrometer. Elemental C, H, N analyses were performed with a Leco Elemental Analyser CHN 900. The ^1H, $^{31}P\{^1H\}$, and $^{13}C\{^1H\}$ NMR spectra were recorded at 200.13, 81.01 and 50.32 MHz, respectively, with a Bruker ACP 200 instrument and a Bruker Avance 300 MHz (300.13 and 121.49 MHz for ^1H and ^{31}P, respectively). ^{31}P chemical shifts were referenced to 85% H_3PO_4 in H_2O, with downfield shifts reported as positive. ^{195}Pt chemical shifts were measured with a Bruker ACP 200 instrument (42.95 MHz) and externally referenced to K_2PtCl_4 in water, with downfield chemical shifts reported as positive. NMR spectra were recorded in pure $CDCl_3$, unless otherwise stated. The presence and amount of CH_2Cl_2 retained in **2a**−**2c**, **2e**, **3c**, **3e** and **6** were determined from the ^1H NMR spectra. The reactions were generally monitored by IR spectroscopy in the ν(CO) region. The isocyanides were obtained from Aldrich and Fluka and were used as received.

Preparation of [$(OC)_4Fe(\mu\text{-dppm})PtCl_2(CNR)$] (2): To a suspension of **1** (409 mg, 0.5 mmol) in CH_2Cl_2) (10 mL), the equivalent amount of CNR was added (over 5 min) in several portions as a solid, or dropwise via a syringe in the case of liquid isocyanides. The resulting clear yellow solution was stirred for a further 10 min, then the solvent was removed affording yellow **2**, in quantitative yields, in sufficient purity for further reactions. If required, **2** can be recrystallized in a refrigerator from a saturated CH_2Cl_2 solution layered with Et_2O or hexane.

2a: Yield: 474 mg. IR (CH_2Cl_2): $\tilde{\nu}$ = 2199 (s) ν(C≡N); 2051 (s), 1978 (m), 1942 (vs), 1936 (sh) ν(CO). ^1H NMR: δ = 1.93 (s, 6 H, xylyl−CH_3), 4.52 (t, 2 H, CH_2, $^3J_{P,H}$ = 11.0 Hz), 6.94−7.92 (m, 23 H, phenyl). $C_{58}H_{31}Cl_2FeNO_4P_2Pt\cdot CH_2Cl_2$ (949.45 + 84.93): calcd. C 45.298, H 3.22, N 1.35; found C 44.89, H 3.02, N 1.20.

2b: Yield: 475 mg. IR (CH_2Cl_2): $\tilde{\nu}$ = 2205 (s) ν(C≡N); 2050 (s), 1971 (m), 1938 (vs), 1928 (sh) ν(CO). ^1H NMR: δ = 3.73 (s, 3 H, OCH_3), 4.53 (t, 2 H, CH_2, $^2J_{P,H}$ = 12.0 Hz), 6.54−7.98 (m, 24 H, phenyl). $C_{37}H_{29}Cl_2FeNO_5P_2Pt\cdot CH_2Cl_2$ (951.42 + 84.93): calcd. C 44.04, H 3.01, N 1.35; found C 44.81, H 3.24, N 1.57.

2c: Yield: 467 mg. IR (CH_2Cl_2): $\tilde{\nu}$ = 2238 (s) ν(C≡N); 2051 (s), 1977 (m), 1938 (vs), 1928 (sh) ν(CO). ^1H NMR: δ = 4.50 (t, 2 H, CH_2, $^2J_{P,H}$ = 11.0 Hz), 4.26 (s, 2 H, NCH_2), 6.99−7.57 (m, 25 H, phenyl). $C_{37}H_{29}Cl_2FeNO_4P_2Pt\cdot CH_2Cl_2$ (935.43 + 84.93): calcd. C 44.73, H 3.06, N 1.37; found C 44.89, H 3.08, N 1.20.

2d: Yield: 463 mg. IR (CH_2Cl_2): $\tilde{\nu}$ = 2205 (s) ν(C≡N); 2050 (s), 1971 (m), 1938 (vs), 1928 (sh) ν(CO). ^1H NMR: δ = 3.73 (s, 3 H, OCH_3), 4.53 (t, 2 H, CH_2, $^2J_{P,H}$ = 12.0 Hz), 6.54−7.98 (m, 24 H, phenyl). $C_{36}H_{33}Cl_2FeNO_4P_2Pt$ (927.44): calcd. C 46.62, H 3.59, N 1.51; found C 46.23, H 3.22, N 1.40.

2e: Yield: 506 mg. IR (CH_2Cl_2): $\tilde{\nu}$ = 2223 (s) ν(C≡N); 2052 (s), 1978 (m), 1943 (vs), 1932 (sh) ν(CO). ^1H NMR: δ = 2.35 (s, 3 H, CH_3), 3.99 (s, 2 H, NCH_2), 4.40 (t, 2 H, CH_2, $^2J_{P,H}$ = 11.2 Hz), 7.21−7.73 (m, 24 H, phenyl). $C_{38}H_{31}Cl_2FeNO_6P_2PtS\cdot 0.5\ CH_2Cl_2$

(1013.53 + 42.47): calcd. C 44.13, H 3.06, N 1.33; found C 44.89, H 3.40, N 1.32.

Preparation of [(OC)$_3$Fe(μ-C=N−R)(μ-dppm)Pt(PPh$_3$)] (3): A solution of an excess of NaBH$_4$ (106 mg, 2.8 mmol) in MeOH (5 mL) was added dropwise to a solution of **2** (0.5 mmol) and PPh$_3$ (131 mg, 0.5 mmol) in CH$_2$Cl$_2$ (15 mL). The orange solution was stirred for 1 h, and the solvents were then removed under reduced pressure. Extraction with CH$_2$Cl$_2$ afforded **3** as yellow-orange solids in moderate yields (50−60%). Analytically pure **3** was obtained by recrystallization in a refrigerator from a saturated CH$_2$Cl$_2$ solution, layered with Et$_2$O or hexane.

3c: Yield: 282 mg, 52%. IR (CH$_2$Cl$_2$): $\tilde{\nu}$ = 1992 (m), 1924 (vs) ν(CO); 1679 (m, br.) ν(C=N). ^{1}H NMR: δ = 3.75 (dt, 2 H, CH$_2$, $^2J_{\mathrm{P,H}}$ = 1.5, 10.0, $^3J_{\mathrm{Pt,H}}$ = 39.8 Hz), 4.90 (s, br., 2 H, NCH$_2$), 6.82−7.55 (m, 40 H, phenyl). C$_{54}$H$_{44}$FeNO$_3$P$_3$Pt·0.5 CH$_2$Cl$_2$ (1098.80 + 42.47): calcd. C 57.36, H 3.97, N 1.23; found C 57.34, H 3.94, N 1.27.

3d: Yield: 305 mg, 56%. IR (CH$_2$Cl$_2$): $\tilde{\nu}$ = 1988 (m), 1921 (vs) ν(CO); 1689 (m, br.) ν(C=N). ^{1}H NMR: δ = 0.82−1.84 (m, 11 H, C$_6$H$_{11}$), 3.71 (t, 2 H, CH$_2$, $^2J_{\mathrm{P,H}}$ = 10.0, $^3J_{\mathrm{Pt,H}}$ = 40.0 Hz), 6.89−7.74 (m, 35 H, phenyl). C$_{53}$H$_{48}$FeNO$_3$P$_3$Pt (1090.82): calcd. C 58.36, H 4.43, N 1.28; found C 58.58, H 4.68, N 1.28.

3e: Yield: 300 mg, 51%. IR (CH$_2$Cl$_2$): $\tilde{\nu}$ = 1996 (m), 1928 (vs) ν(CO); 1648 (m, br.) ν(C=N). ^{1}H NMR: δ = 2.17 (s, 2 H, CH$_3$), 3.75 (t, 2 H, CH$_2$, $^2J_{\mathrm{P,H}}$ =10.0, $^3J_{\mathrm{Pt,H}}$ = 40.3 Hz), 4.88 (s, br., 2 H, NCH$_2$), 6.89−7.55 (m, 40 H, phenyl). C$_{55}$H$_{46}$FeNO$_5$P$_3$PtS·1.5 CH$_2$Cl$_2$ (1176.93 + 127.39): calcd. C 52.03, H 3.79, N 1.07; found C 52.04, H 3.98, N 1.26.

Preparation of [(OC)$_2$FeI(μ-dppm)(μ-CO)PtI(CNR)] (6). Method A: NaI, in a 5-fold excess, was added to a solution of **2** (0.2 mmol) in a mixture of THF/CH$_2$Cl$_2$ (50:50, 10 mL). The initially orange-yellow solution gradually changed to red-violet. After 8 h, all volatiles were removed under reduced pressure. The residue was redissolved in CH$_2$Cl$_2$, NaI and NaCl were filtered off, and the solution concentrated to ca. 5 mL. After layering with heptane, **6** was obtained in the form of air-stable red-violet crystals in yields varying between 50 and 60%. When the reaction was stopped after ca. 1 h by removing all volatiles, the intermediates [(OC)$_4$Fe(μ-dppm)PtI$_2$(CNR)] (**4**) (contaminated by small quantities of **6**) could be isolated after extraction with CH$_2$Cl$_2$, as yellow-orange solids. Selected spectroscopic data for **4c**: IR (ATR): $\tilde{\nu}$ = 2224 (m) ν(C≡N); 2048 (s), 1970 (m), 1940 (vs), 1926 (vs) ν(CO). ^{1}H NMR: δ = 4.71 (t, 2 H, CH$_2$, $^2J_{\mathrm{P,H}}$ = 11.0 Hz), 4.21 (s, 2 H, NCH$_2$), 6.99−7.57 (m, 25 H, phenyl). **4d**: IR (ATR): $\tilde{\nu}$ = 2217 (m) ν(C≡N); 2047 (s), 1968 (m), 1940 (vs), 1927 (vs) ν(CO). **Method B:** An equimolar amount of CNR was added to a solution of **5** (543 mg, 0.5 mmol) in CH$_2$Cl$_2$ (15 mL). The red-violet solution was stirred for 15 min after which all volatiles were removed under reduced pressure affording almost quantitatively pure **6**. If required, **6** can be recrystallized in a refrigerator from a saturated CH$_2$Cl$_2$ solution, layered with heptane.

6a: Yield: 134 mg, 61%. IR (ATR): $\tilde{\nu}$ = 2183 (s) ν(C≡N); 2011 (vs), 1946 (vs), 1844 (m) ν(CO). ^{1}H NMR: δ = 2.50 (s, 6 H, xylyl−CH$_3$), 4.55 (t, 2 H, CH$_2$, $^3J_{\mathrm{P,H}}$ = 12.0 Hz), 6.95−7.86 (m, 23 H, phenyl). C$_{37}$H$_{31}$FeI$_2$NO$_3$P$_2$Pt·CH$_2$Cl$_2$ (1104.34 + 84.93): calcd. C 38.38, H 2.80, N 1.18; found C 38.53, H 2.70, N 1.17.

6b: Yield: 128 mg, 58%. IR (ATR): $\tilde{\nu}$ = 2188 (s) ν(C≡N); 2012 (vs), 1947 (vs), 1840 (m) ν(CO). ^{1}H NMR: δ = 3.85 (s, 3 H, OCH$_3$), 4.64 (t, 2 H, CH$_2$, $^3J_{\mathrm{P,H}}$ = 12.0 Hz), 6.64−7.95 (m, 24 H, phenyl). C$_{36}$H$_{29}$FeI$_2$NO$_5$P$_2$Pt·CH$_2$Cl$_2$ (1105.87 + 84.93): calcd. C 37.31, H 2.62, N 1.18; found C 37.82, H 3.02, N 1.20.

6c: Yield: 133 mg, 61%. IR (ATR): $\tilde{\nu}$ = 2224 (s) ν(C≡N); 2015 (vs), 1944 (vs), 1837 (m) ν(CO). ^{1}H NMR: δ = 4.57 (m, not resolved, 2 H, CH$_2$), 5.07 (s, 2 H, NCH$_2$), 7.08−7.95 (m, 25 H, phenyl). C$_{36}$H$_{29}$FeI$_2$NO$_3$P$_2$Pt·CH$_2$Cl$_2$ (1090.32 + 84.93): calcd. C 37.81, H 2.66, N 1.19; found C 37.94, H 3.04, N 1.25.

6d: Yield: 121 mg, 56%. IR (ATR): $\tilde{\nu}$ = 2213 (s) ν(C≡N); 2008 (vs), 1952 (vs), 1851 (m) ν(CO). ^{1}H NMR: δ = 1.33−2.10 (m, 11 H, C$_6$H$_{11}$), 4.57 (t, 2 H, CH$_2$, $^3J_{\mathrm{P,H}}$ = 11.5 Hz), 7.06−7.87 (m, 20 H, phenyl). C$_{36}$H$_{33}$FeI$_2$NO$_3$P$_2$Pt·CH$_2$Cl$_2$ (1082.35 + 84.93): calcd. C 37.04, H 3.02, N 1.20; found C 37.54, H 3.42, N 1.28.

Collection of the X-ray Data and Structure Determination: Data were collected with a Siemens Stoe AED2 four-circle diffractometer (**3c**) or a Siemens Stoe IPDS (**2d**, **2e**, **6d**) using graphite-monochromated Mo-K_α radiation (λ = 0.71073 Å). The final unit cell parameters were obtained by least squares on the setting angles for 20 reflections with 2Θ = 20−23°. Data were corrected by semi-empirical methods for the absorption correction, using Ψ scans. SHELXS-97 and SHELXL-97 computer programs were used.[39] CCDC-179020 to -179023 contain the supplementary crystallographic data for this paper. These data can be obtained free of charge at www.ccdc.cam.ac.uk/conts/retrieving.html or from the Cambridge Crystallographic Data Centre, 12, Union Road, Cambridge CB2 1EZ, UK [Fax: (internat.) + 44-1223/336-033; E-mail: deposit@ccdc.cam.ac.uk].

Crystal Structure Determination of 2d: Collection of crystallographic data: intensity data were collected using the Ω/2Θ scan mode at 173 K. C$_{36}$H$_{33}$Cl$_2$FeNO$_4$P$_2$Pt (927.41): yellow crystals with approximate dimensions 0.4 × 0.3 × 0.2 mm, triclinic, space group $P\bar{1}$; a = 9.713(2), b = 11.393(3), c = 17.435(6) Å, α = 79.91(4), β = 86.45(3), γ = 70.11(13)°, V = 1786.3(8) Å^3, Z = 2, $\rho_{\mathrm{calcd.}}$ = 1.724 g cm^{-3}, F(000) = 912; 7273 independent reflections in the scan range 4.74° < 2θ < 54°, of which 6567 with $I > 2\sigma(I)$ were used in the structure solution and refinement for 424 parameters; $R1 = \Sigma|F_o - F_c|/\Sigma|F_o|$ = 0.0330 [$I > 2\sigma(I)$], $wR2 = [\Sigma w(F_o^2 - F_c^2)^2/\Sigma wF_o^4]^{1/2}$ = 0.0896 (all data), GoF = 1.052; anisotropic refinement for non-hydrogen atoms; hydrogen atoms in idealized geometries, except for H(1) and H(2), which were refined isotropically. Highest residual electron density 1.764 e·Å^{-3}.

Crystal Structure Determination of 2e: Collection of crystallographic data: intensity data were collected at 293 K. C$_{38.5}$H$_{32}$Cl$_3$FeNO$_6$P$_2$PtS (1055.94): yellow crystals with approximate dimensions 0.2 × 0.3 × 0.4 mm, triclinic, space group $P\bar{1}$; a = 11.178(2), b = 11.245(2), c = 19.578(3) Å, α = 85.392(11), β = 80.148(11), γ = 63.417(10)°, V = 2168.2(5) Å^3, Z = 2, $\rho_{\mathrm{calcd.}}$ = 1.617 g cm^{-3}, F(000) = 1038; 6487 independent reflections in the scan range 4.2° < 2θ < 48.5°, of which 6086 with $I > 2\sigma(I)$ were used in the structure solution and refinement for 488 parameters; $R1 = \Sigma|F_o - F_c|/\Sigma|F_o|$ = 0.0628 [$I > 2\sigma(I)$], $wR2 = [\Sigma w(F_o^2 - F_c^2)^2/\Sigma wF_o^4]^{1/2}$ = 0.1615 (all data), GoF = 1.091; anisotropic refinement for non-hydrogen atoms; hydrogen atoms in idealized geometries. Highest residual electron density 2.278 e·Å^{-3}.

Crystal Structure Determination of 3c: Collection of crystallographic data: intensity data were collected at 293 K. C$_{54.5}$H$_{45}$ClFeNO$_3$P$_3$Pt (1141.21): orange crystals with approximate dimensions 0.2 × 0.3 × 0.35 mm, triclinic, space group $P\bar{1}$; a = 11.713(2), b = 12.779(3), c = 18.798(4) Å, α = 107.03(3), β = 92.26(3), γ = 113.18(3)°, V = 2434(9) Å^3, Z = 2, $\rho_{\mathrm{calcd.}}$ = 1.557 g cm^{-3}, F(000) = 1138; 8562 independent reflections in the scan range $3.62° < 2\theta < 50.0°$, of which 7871 with $I > 2\sigma(I)$ were used in the structure solution and refinement for 594 parameters; $R1 = \Sigma|F_o - F_c|/\Sigma|F_o| = 0.0323$ $[I > 2\sigma(I)]$, $wR2 = [\Sigma w(F_o^2 - F_c^2)^2/\Sigma wF_o^4]^{1/2} = 0.0861$ (all data), $GoF = 1.009$; anisotropic refinement for non-hydrogen atoms; hydrogen atoms in idealized geometries. Highest residual electron density 1.452 e·Å^{-3}.

Crystal Structure Determination of 6d: Collection of crystallographic data: intensity data were collected at 173 K. $C_{36}H_{35}Cl_2FeI_2NO_3P_2Pt$ (1167.23): red violet crystals with approximate dimensions 0.3 × 0.2 × 0.2 mm, monoclinic, space group $P2_1/c$; $a = 15.236(3)$, $b = 11.781(2)$, $b = 22.430(5)$ Å, $\beta = 98.17(3)°$, $V = 3985.4(14)$ Å^3, $Z = 4$, $\rho_{calcd.} = 1.945$ g cm^{-3}, $F(000) = 2224$; 6815 independent reflections in the scan range $4.38° < 2\theta < 50.0°$, of which 5560 with $I > 2\sigma(I)$ were used in the structure solution and refinement for 433 parameters; $R1 = \Sigma|F_o - F_c|/\Sigma|F_o| = 0.0289$ $[I > 2\sigma(I)]$, $wR2 = [\Sigma w(F_o^2 - F_c^2)^2/\Sigma wF_o^4]^{1/2} = 0.0642$ (all data), $GoF = 0.931$; anisotropic refinement for non-hydrogen atoms; hydrogen atoms in idealized geometries. Highest residual electron density 0.994 e·Å^{-3}.

Acknowledgments

The Deutsche Forschungsgemeinschafte, the Ministère de la Recherche et de la Technologie and the Région de Franche-Comté are gratefully thanked for financial support to M. K., H. S. and C. S.

---

[1] D. Sonnenberger, J. D. Atwood, *J. Am. Chem. Soc.* **1980**, *102*, 3484−3489.
[2] W. L. Ingham, N. J. Coville, *Inorg. Chem.* **1992**, *31*, 4084−4090.
[3] R. J. Puddephatt, *Chem. Soc. Rev.* **1983**, *12*, 99−127.
[4] B. Chaudret, B. Delavaux, R. Poilblanc, *Coord. Chem. Rev.* **1988**, *86*, 191−243.
[5] J. T. Mague, *J. Cluster Sci.* **1995**, *6*, 217−269.
[6] *Metal Clusters in Chemisty* (Eds.: P. Braunstein, L. A. Oro, P. R. Raithby), Wiley-VCH, Weinheim, **1999**.
[7] P. Braunstein, J. Rosé, "Catalysis and related reactions with compounds containing heteronuclear metal-metal bonds", in *Comprehensive Organometallic Chemistry II* (Eds.: E. W. Abel, F. G. A. Stone, G. Wilkinson), Elsevier, Oxford, **1995**, p. 351−385.
[8] P. Braunstein, M. Knorr, C. Stern, *Coord. Chem. Rev.* **1998**, *178−180*, 903−965.
[9] N. Wheatley, P. Kalck, *Chem. Rev.* **1999**, *99*, 3379−3420.
[10] L. H. Gade, *Angew. Chem.* **2000**, *112*, 2768−2789; *Angew. Chem. Int. Ed.* **2000**, *39*, 2658−2678.
[11] M. Knorr, C. Strohmann, P. Braunstein, *Organometallics* **1996**, *15*, 5653−5663.
[12] M. Knorr, P. Braunstein, A. Tiripicchio, F. Ugozzoli, *J. Organomet. Chem.* **1996**, *526*, 105−116.
[13] M. Knorr, C. Strohmann, *Eur. J. Inorg. Chem.* **1998**, 495−499.
[14] M. Knorr, C. Strohmann, *Organometallics* **1999**, *18*, 248−257.
[15] M. Knorr, C. Strohmann, *Eur. J. Inorg. Chem.* **2000**, 241−252.
[16] P. Braunstein, M. Knorr, G. Reinhard, U. Schubert, T. Stährfeldt, *Chem. Eur. J.* **2000**, *6*, 4265−4278.
[17] E. Singleton, H. E. Oosthuizen, *Adv. Organomet. Chem.* **1983**, *22*, 209−310.
[18] D. Lentz, *Angew. Chem.* **1994**, *106*, 1377−1393; *Angew. Chem. Int. Ed. Engl.* **1994**, *33*, 1315−1331.
[19] K. S. Ratliff, P. E. Fanwick, C. P. Kubiak, *Polyhedron* **1990**, *9*, 2651−2653.
[20] G. B. Jacobsen, B. L. Shaw, M. Thornton-Pett, *J. Chem. Soc., Dalton Trans.* **1987**, 3079−3083.
[21] X. L. R. Fontaine, G. B. Jacobsen, B. L. Shaw, M. Thornton-Pett, *J. Chem. Soc., Dalton Trans.* **1988**, 741−750.
[22] P. Braunstein, M. Knorr, M. Strampfer, Y. Dusausoy, D. Bayeul, A. DeCian, J. Fischer, P. Zanello, *J. Chem. Soc., Dalton Trans.* **1994**, 1533−1547.
[23] M. Cowie, R. Dickson, *J. Organomet. Chem.* **1987**, *326*, 269−280.
[24] M. E. Tess, P. L. Hill, K. E. Torraca, M. E. Kerr, K. A. Abboud, L. McElwee-White, *Inorg. Chem.* **2000**, *39*, 3942−3944.
[25] D. L. DeLaet, P. E. Fanwick, C. P. Kubiak, *Organometallics* **1986**, *5*, 1807−1811.
[26] M. M. Olmstead, H. Hope, L. S. Benner, A. L. Balch, *J. Am. Chem. Soc.* **1977**, *99*, 5502−5503
[27] J. M. Basset, G. K. Barker, M. Green, J. A. K. Howard, F. G. A. Stone, W. C. Wolsey, *J. Chem. Soc., Dalton Trans.* **1981**, 219−227.
[28] S. L. Schiavo, E. Rotondo, G. Bruno, F. Faraone, *Organometallics* **1991**, *10*, 1613−1620.
[29] B. F. Hoskins, R. J. Steen, T. W. Turney, *J. Chem. Soc., Dalton Trans.* **1984**, 1831−1836.
[30] J. T. Mague, *Inorg. Chem.* **1994**, *13*, 4261−4270.
[31] M. P. Brown, D. Burns, R. Das, P. A. Dolby, M. M. Harding, R. W. Jones, E. J. Robinson, A. K. Smith, *J. Chem. Soc., Dalton Trans.* **1991**, 351−354.
[32] G. K. Anderson, *J. Organomet. Chem.* **1989**, *368*, 385−390.
[33] J. P. Farr, M. M. Olmstead, N. M. Rutherford, F. E. Wood, A. L. Balch, *Organometallics* **1983**, *2*, 1758−1762.
[34] M. E. M. Badley, J. Chatt, R. L. Richards, *J. Chem. Soc. A* **1971**, 21.
[35] R. Bertani, M. Mozzon, F. Benetollo, G. BombierI, R. A. Michelin, *J. Chem. Soc., Dalton Trans.* **1990**, 1197−1205.
[36] K. L. Lu, C. J. Chen, Y. W. Lin, H. W. Gau, F. E. Hong, Y. S. Wen, *Organometallics* **1993**, *12*, 2188−2196.
[37] F. E. Hahn, L. Imhoff, *Organometallics* **1997**, *16*, 763−769.
[38] C. Collazoi, D. Rodewald, H. Schmidt, D. Rheder, *Organometallics* **1996**, *15*, 4884−4887.
[39] G. M. Sheldrick, *SHELXL-97, SHELXS-97*, Universität Göttingen, Germany, **1997**.

Received February 11, 2002
[I02070]